PROCEEDINGS OF SCIENCE

The all-particle spectrum and mean logarithmic mass of cosmic rays in the knee region by LHAASO-KM2A

Hengying Zhang,[a,c,*] **Huihai He**[a,b,c] **and Cunfeng Feng**[d] **for the LHAASO collaboration**

[a] *Key Laboratory of Particle Astrophysics, Institute of High Energy Physics, Chinese Academy of Sciences, 100049 Beijing, China*

[b] *University of Chinese Academy of Sciences, 100049 Beijing, China*

[c] *TIANFU Cosmic Ray Research Center, Chengdu, Sichuan, China*

[d] *Institute of Frontier and Interdisciplinary Science, Shandong University, 266237 Qingdao, Shandong, China*

E-mail: hyzhang@ihep.ac.cn

The kilometer-square array (KM2A) of the Large High Altitude Air Shower Observatory (LHAASO, located at 4410 m above sea level with an atmospheric depth of 600 g/cm^2) can simultaneously measure air shower sizes of both electromagnetic particles and muon contents with high precision for cosmic rays with energies in the knee region. The energy is reconstructed by combining parameters of muons and electromagnetic particles, which is weakly dependent on the mass composition of cosmic rays. We study the measurement method of the all particle spectrum and mean logarithmic mass through the simulation data, and discuss the corresponding systematic errors.

38th International Cosmic Ray Conference (ICRC2023)
26 July - 3 August, 2023
Nagoya, Japan

*Speaker

PoS(ICRC2023)461

1. Introduction

The all-particle energy spectrum of cosmic-rays can be roughly described as a single power law, its energy from 10^9 eV to 10^{20} eV, spanning 11 orders of magnitude, and its flux intensity across more than 30 orders of magnitude. There are four fine structures on the cosmic ray spectrum, namely the "knee" near 4×10^{15} eV, the "second knee" near 4×10^{17} eV, the "ankle" near 4×10^{18} eV, and the GZK cut-off near 10^{20} eV [1]. The origin and propagation mechanism of cosmic rays are revealed through the accurate analysis of the energy spectrum and composition of cosmic rays. Direct detection of cosmic rays have high altitude balloon experiment CREAM, SuperTIGER, etc.; In satellite experiments such as AMS, DAMPE, PAMELA etc., the energy range of cosmic ray detection is mostly below 100 TeV. Due to the rapidly decreasing flux with increasing energy, the study on the composition of cosmic-rays at energies around knee region is difficult for space-born experiments and mainly relies on measurements of the induced extensive air shower (EAS) on ground which suffer from poor composition resolution. A knee structure at few PeV in all-particle energy spectrum of cosmic rays has been observed by many experiments [2–7].

Muons are created in decays of shower hadrons, such as charged pions and kaons. Once produced, muons decouple immediately from the extensive air shower (EAS) and travel almost in straight lines to the detector with smaller attenuation than that for electromagnetic and hadronic particles. Studying muons becomes therefore a sensitive and direct way to probe the hadronic physics and to identify possible deficiencies of hadronic interaction models. The muon number in an EAS is also sensitive to the cosmic ray mass composition. So, the number of muons detected by detectors can be used to determine the composition and energy of the primary particles.

2. Experiment and Simulation

2.1 The LHAASO-KM2A detector

The Large High Altitude Air Shower Observatory (LHAASO) is located in Daocheng, Sichuan, at an altitude of 4410 m [8, 9]. It is a composite detector that includes KM2A with an area of 1.3 km^2 and a water Cherenkov detector array (WCDA) with a total area of 78000 m^2, and 18 wide-field air Cherenkov/fluorescence telescopes (WFCTA). This work uses the KM2A full array, which includes 5216 electromagnetic detectors (EDs) and 1188 muon detectors (MDs). The MD of KM2A is the most powerful muon detector in current CR observatory on the ground, has shown its great ability in the measurement of Crab Nebula in the first phase operation of LHAASO [10]. EDs are distributed with a spacing of 15 m and MDs are distributed with a spacing of 30 m. More details about the experiment setup can be found in [9].

The MD is a pure water Cherenkov detector with an inner diameter of 6.8 m and height of 1.2 m enclosed within a cylindrical concrete tank. An 8-inch PMT sits at the center of the top of the tank and looks downward. The thickness of overburden soil is 2.5 m to absorb the secondary electrons/positrons and gamma-rays in showers[9]. This can reduce the low-energy electromagnetic particles punching through the soil into the water and the threshold for $\mu^{\pm}$ is about 1 GeV[11].

2.2 Monte Carlo Simulation

The simulated data is also for KM2A quarter array, using the Cosmic Ray Simulations for KAscade (CORAIKA) [12] software package to simulate EAS. The high-energy hadronic interaction model is QGSJETII-04 [13] and EPOS-LHC [14], the low energy hadronic interaction model is FLUKA [15]. The zenith angle range of the shower is 0-40 degrees, and the azimuth angle range is 0-360 degrees with energy spectrum $\gamma = -2$ (energy range 10 TeV-50 PeV). MC data contain individual sets for different representative primaries: hydrogen (H), helium (He), nitrogen (denoted by CNO), aluminum (denoted by MgAlSi) and iron (Fe).

The interaction of secondary particles in the detector was simulated by G4KM2A, which was developed in the framework of the GEANT4 package. The sample area was a circular ring region with an inner and outer ring radii of 260 and 480 m, respectively. More details about energy reconstruction can be found in [16]. The total number of simulated events for the five components of the QGSJETII-04 model was approximately 5.555×10^7.

2.3 Data quality Criteria

The operation fetching and reconstruction process of the detector is not completely ideal, and there may be some cases of false trigger and reconstruction error. In order to improve the reconstruction accuracy, the selection criteria are as following:

- $10° <= \theta <= 30°$: zenith angle of shower more than 10 degrees and less than 30 degrees;
- 320m <= R <= 420m: The location of the reconstructed shower core was restricted to inner and outer ring radii of 320 m and 420 m, respectively.
- $N_e > 80$: The number of electromagnetic particles N_e was larger than 80.

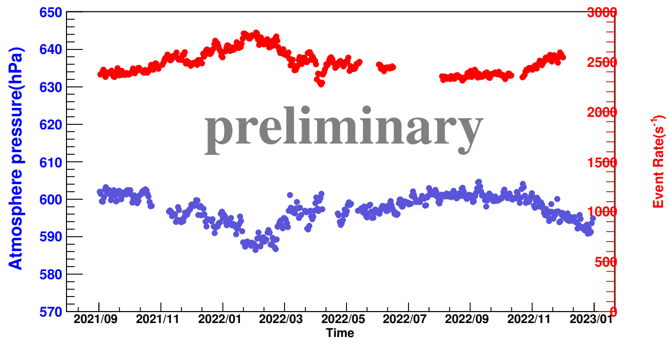

Figure 1: Long time stability of event trigger rate (red) and atmosphere pressure (blue). Each point is an average of data for one day.

The data collected by LHAASO-KM2A array in September 2021 were selected and collected until December 2022. In order to study the performance of the detector, there are many artificial or unexpected factors that may cause data collection anomalies during operation. Therefore, this analysis only uses data files during normal operation. The long-term stability of the ED array event rate is shown in Figure 1.

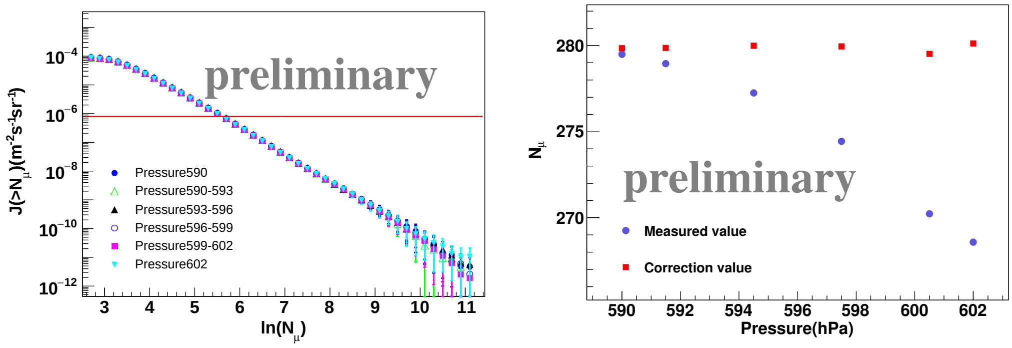

Figure 2: Left: Muon integral intensities for different Pressure intervals derived from the measurements with LHAASO-KM2A. Error bars represent statistical uncertainties. The CIC employed is shown as horizontal red line. Right:After the CIC method, the measured muon content varies with atmospheric pressure. The blue dots are the measured values, and the red squares are the muon content corrected for atmospheric pressure.

Here, we will use the approach based on the Constant Intensity Cut (CIC) method [17, 18], to correct the effect of atmospheric pressure on the experimental data. The aim of the CIC method is to provide a way to relate data from different atmospheric pressure at roughly the same primary energies, without any reference to MC simulations. In order to apply the CIC method, in the first instance, data were grouped into six pressure intervals as shown on the left of Figure 2. The integral muon intensity $J(>N_\mu)$ is estimated according to the differential muon shower size spectrum. The number of muon under different air pressure is obtained after the muon size spectrum in Figure 2 is cut by the intensity $\log_{10}(J)$=-6.1, as shown in the blue dot in Figure 2. Atmospheric pressure data were observed at 4,397m. To be able to study atmospheric changes and apply corrections where needed, the ground pressure at an altitude of 4,397 m is 586.6 hPa (corresponding to simulated atmospheric pressure in CORSIKA atmosphere 1 [19]) as the reference atmosphere pressure. Because the energy reconstruction formula and the mean mass measurement formula are based on the study of showers generated by CORSIKA simulation. By fitting the relationship between the number of muon under different pressure, the ratio relationship between the number of muon under the reference pressure of 586.6hPa and the number of muon under other pressure is obtained, and the number of muon under different pressure is revised to the number of muon under reference pressure. The influence of atmospheric pressure on the measurement of muon content was 4%, and became 0.6% after the correction of atmospheric pressure, as shown on the right of Figure 2.

3. All-Particle Energy Spectrum

To reconstruct the cosmic ray energy weekly dependent of the components, one new parameter $N_{e\mu}$ is developed to reconstruct the primary energy [16], which is defined as:

$$N_{e\mu} = N_e + 2.8N_\mu \tag{1}$$

where N_e(or N_μ) counted only the EDs (or MDs) within 40–200 m far from the shower axis. More details about energy reconstruction can be found in [16].

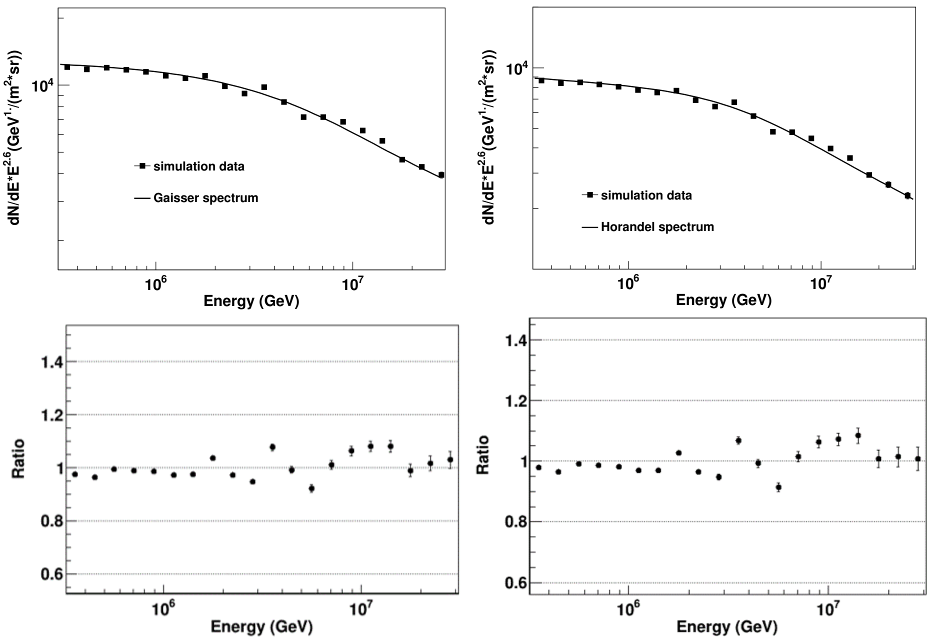

Figure 3: Upper: The points represent the energy spectrum obtained from the analysis of simulation data, and the lines are the real energy spectrum model with Gaisser H3a [20] and Horandel [21] models. Bottom: The ratio of the simulated measured value to the expected value (Gaisser or Horandel) with reconstructed energy.

In order to verify the correctness of the all-particle spectrum measurement method, we use simulated data to check the measurement method. According to the use of different components of the energy spectrum model, after the reconstruction of energy, can reproduce the energy spectrum model? For example, we use the Gaisser [20] energy spectrum model. The points in the Figure 3 represent the energy spectrum obtained from the analysis of simulation data, and the lines are the expected energy spectrum(Gaisser H3a [20] and Horandel [21]). The energy spectrum obtained from the results is consistent with the expected energy spectrum model.

4. Mean logarithmic mass of cosmic rays

According to the Matthews-Heitler model [22], the muon content from a cosmic ray shower is related to its composition. A is the mass number of the cosmic ray nucleus.In the simulation data, according to the relationship between the mean number of muon measured in each energy interval and $\ln(A)$, the mean mass of cosmic ray is derived according to the measured number of muon. Given the energy, the relationship between N_μ and A is $\ln(N_\mu) = p_0 + p_1 \cdot \ln(A)$. The expected truth mean mass of H3a cosmic ray energy model [20] is shown as the black curve in Figure 4, which is the mean mass over five components with the flux as weight. The mean mass (named triggered mass) of the simulation events that passed the event selection is calculated also with the flux weight for each component at each energy interval. This triggered mass matches well with the H3a model. The mean mass (named derived mass) of the simulation events as derived from $\ln(N_\mu)$ is also plotted and this derived mean mass almost totally overlaps with the triggered mean mass.

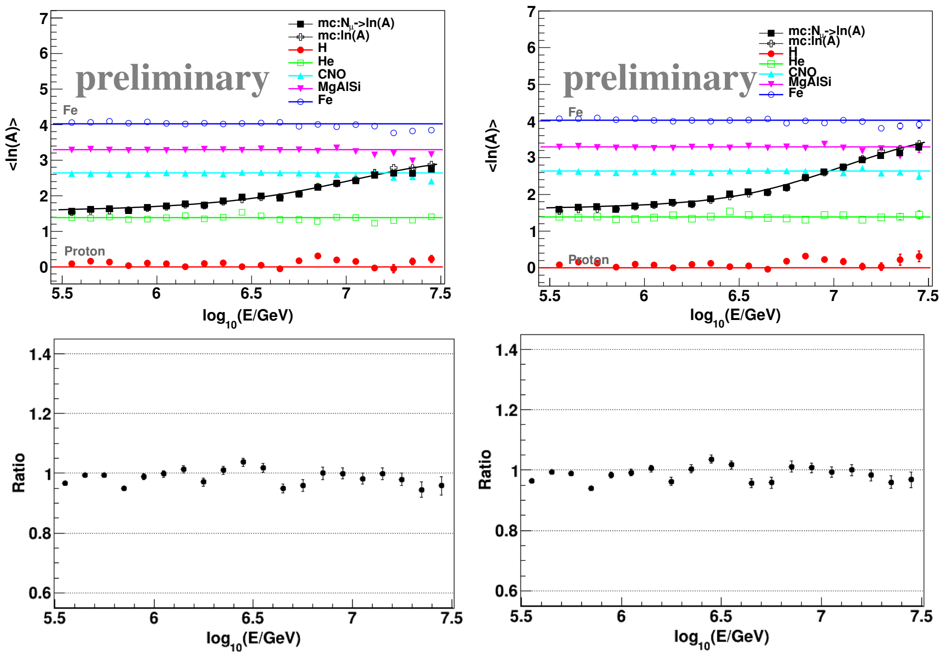

Figure 4: Upper: Mean $\ln(A)$ as a function of the reconstructed energy in a simulation based on the H3a model. The black open-cross (mc:$\ln(A)$) represents the triggered mean logarithmic mass of the simulated showers and the black square represents $\ln(A)$ derived from $\ln(N_\mu)$, and five colors styles represent individual components $\ln(A)$ derived from $\ln(N_\mu)$, respectively. The black curve is the counting result based on the energy according to Ref. [20] and Ref. [21]. The error bars show the statistical uncertainties. Bottom: The ratio of the simulated measured value to the expected value (Gaisser or Horandel) with reconstructed energy.

These plots verify that the mean mass can reliably be derived from the number of muon $\ln(N_\mu)$ within uncertainties.

5. Conclusion

In this work, the data of the KM2A full-array are used to measure the shower muon content and electromagnetic particles of the cosmic rays around the knee region. QGSJETII-04 hadronic interaction model is used to describe the development of showers in the atmosphere, and the interactions in the detector are simulated by a G4KM2A procedure. Simulation data are used to verify the correctness of the all-particle spectrum measurement method. And, we use the simulation data to verify that the mean mass of cosmic rays can be reliably derived from the number of muon $\ln(N_\mu)$ within uncertainties. It provides important support for subsequent physical analysis.

Acknowledgments

We would like to thank all staff members who work at the LHAASO site above 4400 meter above the sea level year round to maintain the detector and keep the water recycling system, electricity power supply and other components of the experiment operating smoothly. We are grateful to Chengdu Management Committee of Tianfu New Area for the constant financial support for research with LHAASO data. This research work is also supported by the following grants: The National Key R & D program of China under grants 2018YFA0404201, 2018YFA0404202 and 2018YFA0404203, 2018YFA0404204, by the National Natural Science Foundation of China(NSFC No.12022502, No.12205314, No. 12105301, No. 12261160362, No.12105294, No.U1931201, No.12175121, No.12275280). We are grateful to Institute of Plateau Meteorology, CMA Chengdu to maintain meteorological data, and in Thailand by the Program Management Unit for Human Resources & Institutional Development, Research and Innovation (PMU-B; B37G660015).

References

[1] J. Blümer, R. Engel and J.R. Hörandel, *Cosmic rays from the knee to the highest energies*, *Progress in Particle and Nuclear Physics* **63** (2009) 293.

[2] Tibet ASγ collaboration, *The All-Particle Spectrum of Primary Cosmic Rays in the Wide Energy Range from 10^{14} to 10^{17} eV Observed with the Tibet-III Air-Shower Array*, *Astrophys. J.* **678** (2008) 1165.

[3] IceCube collaboration, *Cosmic ray spectrum and composition from PeV to EeV using 3 years of data from IceTop and IceCube*, *Phys. Rev. D* **100** (2019) 082002.

[4] T. Antoni et al., *KASCADE measurements of energy spectra for elemental groups of cosmic rays: Results and open problems*, *Astropart. Phys.* **24** (2005) 1.

[5] KASCADE-Grande collaboration, *Measurements of the muon content of EAS in KASCADE-Grande compared with SIBYLL 2.3 predictions*, *Proc. Sci.* **ICRC2017** (2017) 316.

[6] Tunka collaboration, *The Tunka-133 EAS Cherenkov light array: Status of 2011*, *Nucl. Instrum. Methods Phys. Res., Sect. A* **692** (2012) 98.

[7] M. Glasmacher et al., *The cosmic ray composition between 10^{14} and 10^{16} eV*, *Astropart. Phys.* **10** (1999) 291.

[8] LHAASO collaboration, *A future project at tibet: the large high altitude air shower observatory (LHAASO)*, *Chin. Phys. C* **34** (2010) 249.

[9] LHAASO collaboration, *Design of the LHAASO detectors*, *Radiat. Detect. Technol. Methods* **2** (2018) .

[10] LHAASO collaboration, *Observation of the Crab Nebula with LHAASO-KM2A - a performance study*, *Chin. Phys. C* **45** (2021) 025002.

[11] LHAASO collaboration, *Measurement of muonic and electromagnetic components in cosmic ray air showers using LHAASO-KM2A prototype array*, *Phys. Rev. D* **98** (2018) 042001.

[12] D. Heck et al., *corsika: a Monte Carlo code to simulate extensive air showers*, *Forschungszentrum Karlsruhe Report No. FZKA 6019* (1998) .

[13] S. Ostapchenko, *QGSJET-II: physics, recent improvements, and results for air showers*, *EPJ Web Conf.* **52** (2013) 02001.

[14] T. Pierog et al., *EPOS LHC: Test of collective hadronization with data measured at the CERN Large Hadron Collider*, *Phys. Rev. C* **92** (2015) 034906.

[15] G. Battistoni et al., *Overview of the FLUKA code*, *Ann. Nucl. Energy* **82** (2015) 10.

[16] H.Y. Zhang, H.H. He and C.F. Feng, *Approaches to composition independent energy reconstruction of cosmic rays based on the LHAASO-KM2A detector*, *Phys. Rev. D* **106** (2022) 123028.

[17] J. Hersil et al., *Observations of Extensive Air Showers near the Maximum of Their Longitudinal Development*, *Phys. Rev. Lett.* **6** (1961) 22.

[18] W. Apel et al., *Probing the evolution of the EAS muon content in the atmosphere with KASCADE-Grande*, *Astropart. Phys.* **95** (2017) 25.

[19] D. Heck and T. Pierog, *Extensive Air Shower Simulation with CORSIKA: A User's Guide*, *(Karlsruher Institut für Technologie, Karlsruhe, Germany, 2021)* .

[20] T.K. Gaisser et al., *Cosmic ray energy spectrum from measurements of air showers*, *Front. Phys.* **8** (2013) 748.

[21] Jörg R. Hörandel, *On the knee in the energy spectrum of cosmic rays*, *Astropart. Phys.* **19** (2003) 193.

[22] J. Matthews, *A heitler model of extensive air showers*, *Astropart. Phys.* **22** (2005) 387 .

Full Authors List: LHAASO Collaboration

Zhen Cao[1,2,3], F. Aharonian[4,5], Q. An[6,7], Axikegu[8], Y.X. Bai[1,3], Y.W. Bao[9], D. Bastieri[10], X.J. Bi[1,2,3], Y.J. Bi[1,3], J.T. Cai[10], Q. Cao[11], W.Y. Cao[7], Zhe Cao[6,7], J. Chang[12], J.F. Chang[1,3,6], A.M. Chen[13], E.S. Chen[1,2,3], Liang Chen[14], Lin Chen[8], Long Chen[8], M.J. Chen[1,3], M.L. Chen[1,3,6], Q.H. Chen[8], S.H. Chen[1,2,3], S.Z. Chen[1,3], T.L. Chen[15], Y. Chen[9], N. Cheng[1,3], Y.D. Cheng[1,3], M.Y. Cui[12], S.W. Cui[11], X.H. Cui[16], Y.D. Cui[17], B.Z. Dai[18], H.L. Dai[1,3,6], Z.G. Dai[7], Danzengluobu[15], D. della Volpe[19], X.Q. Dong[1,2,3], K.K. Duan[12], J.H. Fan[10], Y.Z. Fan[12], J. Fang[18], K. Fang[1,3], C.F. Feng[20], L. Feng[12], S.H. Feng[1,3], X.T. Feng[20], Y.L. Feng[15], S. Gabici[21], B. Gao[1,3], C.D. Gao[20], L.Q. Gao[1,2,3], Q. Gao[15], W. Gao[1,3], W.K. Gao[1,2,3], M.M. Ge[18], L.S. Geng[1,3], G. Giacinti[13], G.H. Gong[22], Q.B. Gou[1,3], M.H. Gu[1,3,6], F.L. Guo[14], X.L. Guo[8], Y.Q. Guo[1,3], Y.Y. Guo[12], Y.A. Han[23], H.H. He[1,2,3], H.N. He[12], J.Y. He[12], X.B. He[17], Y. He[8], M. Heller[19], Y.K. Hor[17], B.W. Hou[1,2,3], C. Hou[1,3], X. Hou[24], H.B. Hu[1,2,3], Q. Hu[7,12], S.C. Hu[1,2,3], D.H. Huang[8], T.Q. Huang[1,3], W.J. Huang[17], X.T. Huang[20], X.Y. Huang[12], Y. Huang[1,2,3], Z.C. Huang[8], X.L. Ji[1,3,6], H.Y. Jia[8], K. Jia[20], K. Jiang[6,7], X.W. Jiang[1,3], Z.J. Jiang[18], M. Jin[8], M.M. Kang[25], T. Ke[1,3], D. Kuleshov[26], K. Kurinov[26,27], B.B. Li[11], Cheng Li[6,7], Cong Li[1,3], D. Li[1,2,3], F. Li[1,3,6], H.B. Li[1,3], H.C. Li[1,3], H.Y. Li[7,12], J. Li[7,12], Jian Li[7], Jie Li[1,3,6], K. Li[1,3], W.L. Li[20], W.L. Li[13], X.R. Li[1,3], Xin Li[6,7], Y.Z. Li[1,2,3], Zhe Li[1,3], Zhuo Li[28], E.W. Liang[29], Y.F. Liang[29], S.J. Lin[17], B. Liu[7], C. Liu[1,3], D. Liu[20], H. Liu[8], H.D. Liu[23], J. Liu[1,3], J.L. Liu[1,3], J.Y. Liu[1,3], M.Y. Liu[15], R.Y. Liu[9], S.M. Liu[8], W. Liu[1,3], Y. Liu[10], Y.N. Liu[22], R. Lu[18], Q. Luo[17], H.K. Lv[1,3], B.Q. Ma[28], L.L. Ma[1,3], X.H. Ma[1,3], J.R. Mao[24], Z. Min[1,3], W. Mitthumsiri[30], H.J. Mu[23], Y.C. Nan[1,3], A. Neronov[21], Z.W. Ou[17], B.Y. Pang[8], P. Pattarakijwanich[30], Z.Y. Pei[10], M.Y. Qi[1,3], Y.Q. Qi[11], B.Q. Qiao[1,3], J.J. Qin[7], D. Ruffolo[30], A. Sáiz[30], D. Semikoz[21], C.Y. Shao[17], L. Shao[11], O. Shchegolev[26,27], X.D. Sheng[1,3], F.W. Shu[31], H.C. Song[28], Yu.V. Stenkin[26,27], V. Stepanov[26], Y. Su[12], Q.N. Sun[8], X.N. Sun[29], Z.B. Sun[32], P.H.T. Tam[17], Q.W. Tang[31], Z.B. Tang[6,7], W.W. Tian[2,16], C. Wang[32], C.B. Wang[8], G.W. Wang[7], H.G. Wang[10], H.H. Wang[17], J.C. Wang[24], K. Wang[9], L.P. Wang[20], L.Y. Wang[1,3], P.H. Wang[8], R. Wang[20], W. Wang[17], X.G. Wang[29], X.Y. Wang[9], Y. Wang[8], Y.D. Wang[1,3], Y.J. Wang[1,3], Z.H. Wang[25], Z.X. Wang[18], Zhen Wang[13], Zheng Wang[1,3,6], D.M. Wei[12], J.J. Wei[12], Y.J. Wei[1,2,3], T. Wen[18], C.Y. Wu[1,3], H.R. Wu[1,3], S. Wu[1,3], X.F. Wu[12], Y.S. Wu[7], S.Q. Xi[1,3], J. Xia[7,12], J.J. Xia[8], G.M. Xiang[2,14], D.X. Xiao[11], G. Xiao[1,3], G.G. Xin[1,3], Y.L. Xin[8], Y. Xing[14], Z. Xiong[1,2,3], D.L. Xu[13], R.F. Xu[1,2,3], R.X. Xu[28], W.L. Xu[25], L. Xue[20], D.H. Yan[18], J.Z. Yan[12], T. Yan[1,3], C.W. Yang[25], F. Yang[11], F.F. Yang[1,3,6], H.W. Yang[17], J.Y. Yang[17], L.L. Yang[17], M.J. Yang[1,3], R.Z. Yang[7], S.B. Yang[18], Y.H. Yao[25], Z.G. Yao[1,3], Y.M. Ye[22], L.Q. Yin[1,3], N. Yin[20], X.H. You[1,3], Z.Y. You[1,2,3], Y.H. Yu[7], Q. Yuan[12], H. Yue[1,2,3], H.D. Zeng[12], T.X. Zeng[1,3,6], W. Zeng[18], M. Zha[1,3], B.B. Zhang[9], F. Zhang[8], H.M. Zhang[9], H.Y. Zhang[1,3], J.L. Zhang[16], L.X. Zhang[10], Li Zhang[18], P.F. Zhang[18], P.P. Zhang[7,12], R. Zhang[7,12], S.B. Zhang[2,16], S.R. Zhang[11], S.S. Zhang[1,3], X. Zhang[9], X.P. Zhang[1,3], Y.F. Zhang[8], Yi Zhang[1,12], Yong Zhang[1,3], B. Zhao[8], J. Zhao[1,3], L. Zhao[6,7], L.Z. Zhao[11], S.P. Zhao[12,20], F. Zheng[32], B. Zhou[1,3], H. Zhou[13], J.N. Zhou[14], M. Zhou[31], P. Zhou[9], R. Zhou[25], X.X. Zhou[8], C.G. Zhu[20], F.R. Zhu[8], H. Zhu[16], K.J. Zhu[1,2,3,6], X. Zuo[1,3]

[1] Key Laboratory of Particle Astrophysics & Experimental Physics Division & Computing Center, Institute of High Energy Physics, Chinese Academy of Sciences, 100049 Beijing, China
[2] University of Chinese Academy of Sciences, 100049 Beijing, China
[3] TIANFU Cosmic Ray Research Center, Chengdu, Sichuan, China
[4] Dublin Institute for Advanced Studies, 31 Fitzwilliam Place, 2 Dublin, Ireland
[5] Max-Planck-Institut for Nuclear Physics, P.O. Box 103980, 69029 Heidelberg, Germany
[6] State Key Laboratory of Particle Detection and Electronics, China
[7] University of Science and Technology of China, 230026 Hefei, Anhui, China
[8] School of Physical Science and Technology & School of Information Science and Technology, Southwest Jiaotong University, 610031 Chengdu, Sichuan, China
[9] School of Astronomy and Space Science, Nanjing University, 210023 Nanjing, Jiangsu, China
[10] Center for Astrophysics, Guangzhou University, 510006 Guangzhou, Guangdong, China
[11] Hebei Normal University, 050024 Shijiazhuang, Hebei, China
[12] Key Laboratory of Dark Matter and Space Astronomy & Key Laboratory of Radio Astronomy, Purple Mountain Observatory, Chinese Academy of Sciences, 210023 Nanjing, Jiangsu, China
[13] Tsung-Dao Lee Institute & School of Physics and Astronomy, Shanghai Jiao Tong University, 200240 Shanghai, China
[14] Key Laboratory for Research in Galaxies and Cosmology, Shanghai Astronomical Observatory, Chinese Academy of Sciences, 200030 Shanghai, China
[15] Key Laboratory of Cosmic Rays (Tibet University), Ministry of Education, 850000 Lhasa, Tibet, China
[16] National Astronomical Observatories, Chinese Academy of Sciences, 100101 Beijing, China
[17] School of Physics and Astronomy (Zhuhai) & School of Physics (Guangzhou) & Sino-French Institute of Nuclear Engineering and Technology (Zhuhai), Sun Yat-sen University, 519000 Zhuhai & 510275 Guangzhou, Guangdong, China
[18] School of Physics and Astronomy, Yunnan University, 650091 Kunming, Yunnan, China
[19] Département de Physique Nucléaire et Corpusculaire, Faculté de Sciences, Université de Genève, 24 Quai Ernest Ansermet, 1211 Geneva, Switzerland
[20] Institute of Frontier and Interdisciplinary Science, Shandong University, 266237 Qingdao, Shandong, China
[21] APC, Universit'e Paris Cit'e, CNRS/IN2P3, CEA/IRFU, Observatoire de Paris, 119 75205 Paris, France
[22] Department of Engineering Physics, Tsinghua University, 100084 Beijing, China
[23] School of Physics and Microelectronics, Zhengzhou University, 450001 Zhengzhou, Henan, China
[24] Yunnan Observatories, Chinese Academy of Sciences, 650216 Kunming, Yunnan, China
[25] College of Physics, Sichuan University, 610065 Chengdu, Sichuan, China

PoS(ICRC2023)461

[26] Institute for Nuclear Research of Russian Academy of Sciences, 117312 Moscow, Russia
[27] Moscow Institute of Physics and Technology, 141700 Moscow, Russia
[28] School of Physics, Peking University, 100871 Beijing, China
[29] School of Physical Science and Technology, Guangxi University, 530004 Nanning, Guangxi, China
[30] Department of Physics, Faculty of Science, Mahidol University, 10400 Bangkok, Thailand
[31] Center for Relativistic Astrophysics and High Energy Physics, School of Physics and Materials Science & Institute of Space Science and Technology, Nanchang University, 330031 Nanchang, Jiangxi, China
[32] National Space Science Center, Chinese Academy of Sciences, 100190 Beijing, China